

Observation of Resonant Transfer and Excitation to Specific *LS*-Coupled States in $O^{5+} + He$ Collisions by High-Resolution, 0° Auger-Electron Spectroscopy

J. K. Swenson,^(a) Y. Yamazaki,^(b) P. D. Miller, H. F. Krause, P. F. Dittner, P. L. Pepmiller, S. Datz, and N. Stolterfoht^(c)

Oak Ridge National Laboratory, Oak Ridge, Tennessee 37831

(Received 21 July 1986)

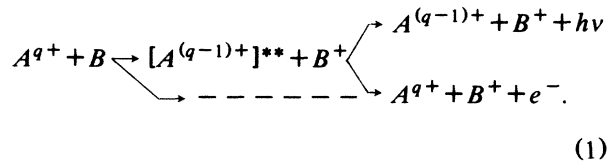
Conclusive evidence is presented for resonant transfer and excitation to specific intermediate states in collisions of Li-like O^{5+} with He. Using the technique of high-resolution 0° Auger-electron spectroscopy, we observed a maximum in the cross section for production of Be-like $1s2s2p^2^3D$ and $1s2s2p^2^1D$ states as a function of incident ion energy. The peak appears at ~ 13 MeV with a width of ~ 7 MeV and is in good agreement with the impulse-approximation model for resonant transfer and excitation.

PACS numbers: 34.50.Fa, 34.50.Pi, 34.70.+e

Resonant transfer and excitation^{1,2} (RTE) has received a great deal of attention over the past five years, both for its relationship to dielectronic recombination and as a basic mechanism in ion-atom collision physics. Just as radiative electron capture³ is the ion-atom collision analog of the inverse photoelectric effect for free electrons, RTE is the collision analog of the inverse Auger effect.

RTE may be viewed, from the projectile frame, as the collision of a loosely bound target electron with an electron bound to the projectile in which the projectile electron is excited and the loosely bound electron thereby loses just enough energy to be transferred to the projectile, forming a doubly excited state. If the transferred electron were in fact free (inverse Auger effect), this would be a sharply resonant process and would occur at an electron collision energy ϵ_r equal to the Auger transition energy ϵ_a for that doubly excited state. Since this electron is bound to the target atom, it has an intrinsic momentum distribution along the collision axis (the Compton profile). This shifts the resonance energy ϵ_r by the ratio of the projectile to electron mass, to a collision energy $E_r = \epsilon_r M/m$, and smears out the resonance over several megaelectronvolts in collision energy.

Equation (1) illustrates the more general transfer plus excitation (TE) process in which an electron is transferred from the target to the projectile-ion and a core electron in the projectile is excited:



The doubly excited intermediate state may be formed through electron-electron interactions described above or from two clearly independent events, e.g., nuclear Coulomb excitation of the electron bound to the projectile ion plus electron transfer in the same collision. The latter process is referred to as nonresonant transfer and

excitation (NTE).⁴

The doubly excited state of Eq. (1) may then decay via emission of a photon or through reemission of an Auger electron. The similarity with dielectronic recombination results when radiative decay occurs. However, for low- Z ions ($Z < 20$) and low- n states, electron emission will be the dominant decay mode. For these systems, it is desirable to study the RTE process through the Auger decay channel.

Up to now, the RTE process has been studied almost exclusively through x-ray, charge-changed-beam coincidence techniques.⁵ In these experiments projectile ions which had captured one electron were detected in coincidence with projectile K x rays. The energy resolution of the x-ray detector was sufficient to resolve $K\alpha$ and $K\beta$ x rays; thus they were able to distinguish simultaneous capture and excitation events involving the $n=2$ shell from those events which involved shells with $n \geq 3$.

Pepmiller *et al.*⁶ used high-resolution x-ray spectroscopy to study F^{8+} collisions with He, Ne, and Ar. Their results showed only an NTE contribution to the cross section for formation of doubly excited F^{7+} ions in the $2s2p$ and $2p^2$ configurations and no significant RTE contribution. However, the resolution of that experiment was insufficient to resolve the different multiplets, e.g., the $2p^2^1D$ and $2p^2^3P$ states, which were each expected to have different RTE and NTE contributions.

High-resolution Auger-electron measurements of the TE process were made by Itoh *et al.*⁷ for the $He^+ + He$ collision system. It was proposed that the $2p^2^1D$ state was being populated through the RTE mechanism, but this interpretation involved difficulties since the width of the resonance feature was found to be narrower than the He $1s$ electron's Compton profile would permit. Straten and Morgenstern⁸ have attempted to explain their results by showing that the observed energy dependence of the production of the $2p^2^1D$ state could be reproduced by taking into account post-collision interactions and interferences between the $2p^2^1D$ and the $2s2p^1P$ autoionizing states.

In this Letter, we present conclusive evidence that RTE is proceeding through specific resolved intermediate states. Our results show that RTE is an important mechanism in the production of Be-like doubly excited states in energetic collisions of Li-like O^{5+} ions incident on He. Using high-resolution 0° Auger spectroscopy, we have measured the cross sections for the production of Auger electrons from the decay of the $1s2s2p^2\ ^3D$ and $1s2s2p^2\ ^1D$ states in O^{4+} to the $1s^22s^2\ ^2S$ ground state of O^{5+} as a function of the incident ion energy. We observe a resonance in these cross sections with a maximum at 13 MeV and a full width at half maximum of 7 MeV. These results are in good agreement with Brandt's impulse-approximation model for RTE.¹ The RTE resonance features are observed to be superimposed upon a monotonic NTE-Auger background.

The experiment was performed at the EN Tandem Van de Graaff facility at Oak Ridge National Laboratory with the high-resolution electron spectrometer and target chamber temporarily transported from the Hahn-Meitner Institut, Berlin. Details of the experimental apparatus and the technique of high-resolution 0° electron spectroscopy have been given previously.⁹ 5- to 25-MeV oxygen ions were stripped after acceleration and O^{5+} ions were magnetically selected from the emerging charge-state distributions. These ions were collimated and sent through a He gas cell. The beam then passed through the first stage of a tandem 90° parallel-plate electron spectrometer⁹ where electrons emitted at 0° to the beam axis were deflected out of the beam. These electrons were then decelerated in front of the second stage where they were energy analyzed in high resolution. The undeflected ion beam was collected and integrated in a suppressed Faraday cup. The chamber base pressure was 1×10^{-6} Torr, and was 4×10^{-4} Torr with 20 mTorr of He in the cell. The Auger-electron yield was found to be linear with He pressure, thus ensuring single-collision conditions. In this experiment, Auger electrons were decelerated to a constant pass energy of 50 eV which resulted in a typical energy resolution of $\Delta E/E = 0.2\%$.

Figure 1 shows a series of high-resolution 0° Auger-electron spectra for $O^{5+} + He$, after background subtraction and transformation into the projectile frame, for various incident beam energies. Line assignments were made by use of the calculations of Bruch *et al.*¹⁰ Very high-resolution spectra ($\Delta E/E < 0.1\%$) were acquired prior to these measurements for a series of incident charge states of O^{q+} to help unfold the complex structure of the spectra shown in Fig. 1.

We shall focus our attention on the Be-like $1s2s2p^2\ ^3D$ and $1s2s2p^2\ ^1D$ states which are formed when O^{5+} ions capture a target electron and, in the same collision, are excited into an autoionizing state. Auger-electron emission will occur with $\sim 99\%$ probability and result in decay to either the $1s^22s^2\ ^2S$ ground state or the $1s^22p^2\ ^2P$

state with a branching ratio for decay to the ground state of 0.9 and 0.4 for the 3D and 1D states, respectively (see Table I). The Auger lines which result from the decay of these two states to the ground state are shown as shaded peaks in Fig. 1 in the 5-MeV spectrum.

First, we call attention to the asymmetric Fano line shape¹² observed for the $1s2s2p^2\ ^3D$ state for ion energies 10 to 15 MeV. This results from the interference in the amplitudes for electrons produced via the TE mechanism and for continuum electrons produced through

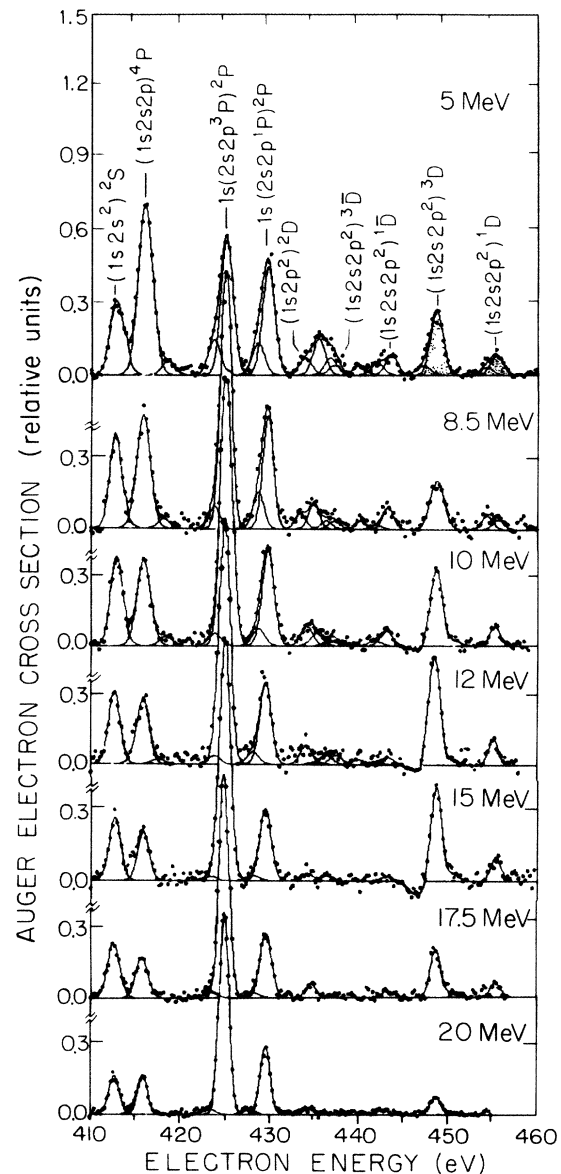


FIG. 1. High-resolution Auger-electron spectra for $O^{5+} + He$ for various incident ion energies. The $1s2s2p^2\ ^3D$ and 1D states refer to decay to the ionic ground state $1s^22s^2\ ^2S$, whereas the $1s2s2p^2\ ^3\bar{D}$ and $^1\bar{D}$ states refer to decay to the $1s^22p^2\ ^2P$ final state.

TABLE I. Calculated values (Ref. 11) for σ_{RC} for $e + O^{5+}(1s^2 2s) \rightarrow O^{4+}(1s 2s 2p^2)$ averaged over an energy interval of $\Delta\epsilon = 1$ Ry. The barred states refer to decay to the $O^{5+}(1s^2 2p)$ final state, whereas the unbarred states refer to the $O^{5+}(1s^2 2s)$ ground state. ξ and ω are the calculated Auger and fluorescence yields, respectively. Resonant-excitation cross sections $\sigma_{RE} = \xi\sigma_{RC}$, in units of 10^{-20} cm², are given in comparison with our experimental results.

| State ($1s 2s 2p^2$) | ξ | ω | σ_{RC} | σ_{RE}^a | σ_{RE}^b |
|---------------------------|-------|----------|---------------|-----------------|-----------------|
| $^1\bar{D}$ | 0.584 | | | 5.2 | |
| 1D | 0.409 | 0.0073 | 8.86 | 3.6 | 8.7 |
| $^3\bar{D}$ | 0.085 | | | 2.3 | |
| 3D | 0.899 | 0.0160 | 26.7 | 24 | 35 |

^aTheory, Ref. 11.

^bThis experiment.

direct ionization of the target [as represented by the dashed line in Eq. (1)]. We note that at the beam energy where RTE has a maximum cross section, the centroid of the energy distribution of the binary-encounter electrons¹³ is equal to that of the RTE Auger electrons ejected at 0°. As we move away from this ion energy, there is more of a mismatch between the Auger energy and the centroid energy of the binary-encounter peak, and it is interesting to note that the interference effect decreases.

In Fig. 2, the integrated cross sections, if we assume isotropy in the projectile frame, for Auger decay of the $1s 2s 2p^2 {}^3D$ and 1D states to the ionic ground state $1s^2 2s^2 S$, are shown in comparison with calculations of the cross section for RTE followed by Auger-electron emission (RTEA). By use of the impulse-approximation model for RTE,¹ the RTEA cross section for a particular intermediate state with a resonance energy ϵ_r [Eq. (23), Ref. 1] can be written as

$$\sigma_{RTEA} = \xi(M/2E)^{1/2} \sigma_{RC} \sum_i J_i(p_{iz}'), \quad (2)$$

where ξ is the Auger yield for the selected decay channel, σ_{RC} is the cross section for radiationless capture into a particular intermediate state averaged over an energy interval of 1 Ry,¹¹ M and E are the ion mass and incident energy, respectively, and $\sum_i J_i(p_{iz}')$ is the probability that the i th electron in the target has a momentum $p_{iz}' = (\epsilon_r - Em/M)(M/2E)^{1/2}$ along the z (beam) direction (the Compton profile), summed over all target electrons. For a He target \sum_i is replaced by a 2 for the two He $1s$ electrons.

The RTEA cross sections were obtained with use of Eq. (2) and the values for σ_{RC} and ξ for the $1s 2s 2p^2 {}^3D$ and 1D states in oxygen,¹¹ given in Table I. The dashed curve in Fig. 2 is the resulting 3D RTEA calculation multiplied by a factor of 1.45. This is superimposed

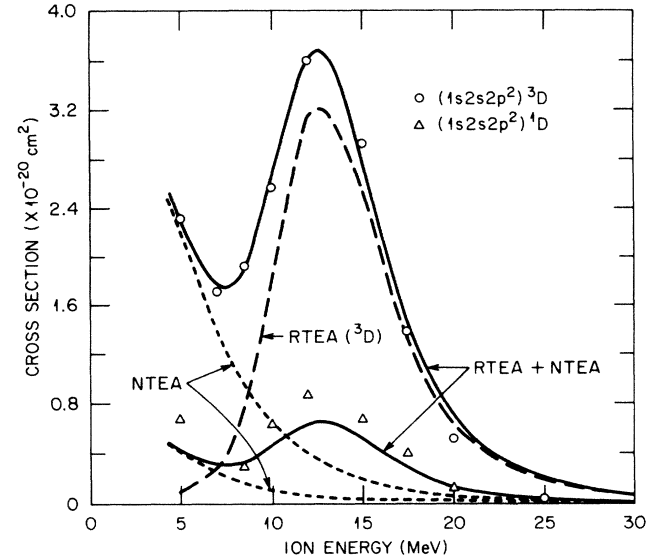


FIG. 2. Cross sections for Auger decay of the $1s 2s 2p^2 {}^3D$ and the $1s 2s 2p^2 {}^1D$ states to the $1s^2 2s^2 S$ ground state following collisions of $O^{5+} + He$. The upper solid curve is an impulse-approximation-model calculation for RTE followed by Auger decay, for the 3D state (dashed curve), superimposed on an underlying NTE-Auger background (dotted curve). The lower solid curve is the corresponding calculation for the 1D state.

upon a monotonic NTE-Auger (NTEA) background (dotted curve). This curve agrees with an NTEA calculation⁴ multiplied by 0.7, for the energy region above 8 MeV. A similar calculation was done for the 1D state with use of Table I and the same scaling factors, and is shown as the lower solid curve in Fig. 2. Relative uncertainties in the data are $\pm 10\%$ and are due to background subtraction and peak fits. Absolute uncertainties in the data are $\pm 30\%$. Uncertainties in the calculated RTEA cross sections are $\pm 30\%$ and are due to uncertainties in the scaling factors and in the quantities listed in Table I.¹⁴

The good agreement between the energy dependence of the 3D cross section and the scaled calculation for RTEA indicates that the impulse-approximation model can be used to describe the RTE process for this collision system. Therefore we may extract from Eq. (2) the product $\xi\sigma_{RC} = \sigma_{RE}$ (the resonant excitation cross section)¹¹ and make a direct comparison with our experiment. On the basis of the RTEA scaling factor, we find $\sigma_{RE}({}^3D) = 3.5 \times 10^{-19}$ cm² compared to the value of 2.4×10^{-19} cm² given in Table I.

We see that the predicted cross section for the 1D state (lower solid curve) underestimates the measured 1D cross sections by $\sim 30\%$. If we consider the degree of uncertainty associated with the decay rates for these states,¹⁴ our results are not entirely inconsistent with the calculation. We find a ratio of the 3D to 1D RTEA cross

sections to be ~ 4 , whereas the calculated ratio is 6.6. Thus $\sigma_{\text{RE}}(^1D) = 8.7 \times 10^{-20} \text{ cm}^2$, compared to $3.6 \times 10^{-20} \text{ cm}^2$ as given in Table I.

An important aspect of the results presented here is that high-resolution Auger spectroscopy provides detailed information concerning both the target and the projectile when the impulse-approximation model can be used to describe RTE. The shape and width of the RTE resonance feature is directly related to the Compton profile of the target electrons. Measurement of RTEA cross sections for individual states provides a direct comparison between experiment and theory.

Future studies of RTE for other systems such as $\text{C}^{3+} + \text{He}$ would be useful. For this more symmetric case, discrepancies between the impulse-approximation model and experiment, which are evident for the $\text{He}^+ + \text{He}$ system,⁷ may begin to appear. It is clear that for those cases where the impulse approximation is not valid, a more complete theoretical treatment of RTE (and NTE) is needed. High-resolution Auger-electron measurements for these systems could give detailed information on the collision process and thus provide stringent tests of the models used to describe phenomena such as RTE.

The authors would like to thank Dr. Stephen Shafroth for his support and helpful discussions during this work. This work was supported by the U.S. Department of Energy, Division of Basic Energy Sciences, under Contract No. DE-AC05-84OR21400 with Martin Marietta Energy Systems, Inc. and the Division of Chemical Sciences under Contract No. DE-AS05-78ER06027.

^(a)Guest from University of North Carolina, Department of Physics, Chapel Hill, NC 17514. Present address: Oak Ridge National Laboratory, Oak Ridge, TN 37831.

^(b)Permanent address: Research Laboratory for Nuclear

Reactors, Tokyo Institute of Technology, Tokyo, Japan.

^(c)Permanent address: Hahn-Meitner Institute für Kernforschung Berlin, D-1000 Berlin 39, West Germany.

¹D. Brandt, Phys. Rev. A **27**, 1314 (1983).

²In this Letter we use the convention that RTE refers only to the formation of the intermediate state (Ref. 1). RTE followed by Auger emission or x-ray emission will be designated RTEA or RTEEX, respectively.

³H. D. Betz, in *Atomic Physics: Accelerators*, edited by Patrick Richard, Methods of Experimental Physics Vol. 17 (Academic, New York, 1980), pp. 73–148.

⁴D. Brandt, Nucl. Instrum. Methods Phys. Res. **214**, 93 (1983).

⁵J. A. Tanis, E. M. Bernstein, W. G. Graham, M. Clark, S. M. Shafroth, B. M. Johnson, K. W. Jones, and M. Meron, Phys. Rev. Lett. **49**, 1325 (1982); J. A. Tanis, E. M. Bernstein, W. G. Graham, M. P. Stockli, M. Clark, R. H. McFarland, T. J. Morgan, K. H. Berkner, A. S. Schlachter, and J. W. Stearns, Phys. Rev. Lett. **53**, 2551 (1984); M. Clark, D. Brandt, J. K. Swenson, and S. M. Shafroth, Phys. Rev. Lett. **54**, 544 (1985). These authors use the term RTE to include subsequent x-ray decay of the intermediate state. We call this process RTEEX.

⁶P. L. Pepmiller, P. Richard, J. Newcomb, J. Hall, and T. R. Dillingham, Phys. Rev. A **31**, 734 (1985).

⁷A. Itoh, T. J. M. Zouros, D. Schneider, U. Stettner, W. Zeitz, and N. Stolterfoht, J. Phys. B **18**, 4581 (1985).

⁸P. van der Straten and R. Morgenstern, J. Phys. B **19**, 1361 (1986).

⁹A. Itoh, D. Schneider, T. Schneider, T. J. M. Zouros, G. Nolte, G. Schiwietz, W. Zeitz, and N. Stolterfoht, Phys. Rev. A **31**, 684 (1985).

¹⁰R. Bruch, D. Schneider, W. H. E. Schwarz, M. Meinhardt, B. M. Johnson, and K. Taulbjerg, Phys. Rev. A **19**, 587 (1979).

¹¹Y. Hahn, Phys. Lett. A (to be published).

¹²U. Fano, Phys. Rev. **124**, 1866 (1961).

¹³N. Stolterfoht, in *Structure and Collision of Ions and Atoms*, edited by I. A. Sellin, Topics in Current Physics Vol. 5 (Springer-Verlag, New York, 1978), pp. 155–199.

¹⁴Y. Hahn, private communication.